Progress In Electromagnetics Research C, Vol. 60, 95–103, 2015

Wideband Printed Planar Monopole Antenna for PCS, UWB and X-Band Applications

Goksenin Bozdag* and Alp Kustepeli

Abstract—In this paper, a printed planar monopole antenna (PPMA) is presented for PCS, UWB and X-band. The antenna is designed in two stages. In the design of the preliminary PPMA used to obtain the proposed PPMA, the structure is divided into sections, and they are optimized in the sense of bottom to up strategy. The bandwidth is enhanced by employing tapered transitions and inset feed. The resulting antenna operates between 2.37 GHz and 12 GHz with VSWR < 2 and an average peak realized gain of 4.95 dB. Therefore, the preliminary antenna can be considered to be suitable for Bluetooth, WLAN, WiMAX, UWB and X-band. The proposed PPMA is designed by implementing slots on the preliminary PPMA to include PCS, and to suppress Bluetooth and commonly used WLAN and WiMAX bands, the ones allocated out of UWB. The proposed antenna operates in the 1.67 GHz–1.91 GHz and 3 GHz–15 GHz bands with VSWR < 2. The peak realized gain (G_{pr}) in PCS is 1.32 dB at 1.8 GHz, and the average G_{pr} is 5 dB for the 3 GHz–15 GHz band. The group delay performances are also examined, and the maximum group delay deviations of preliminary and proposed PPMAs are observed as 1 ns and 1.25 ns, respectively.

1. INTRODUCTION

In recent years, the growth in wireless communication technologies has led to development of various wireless systems such as PCS, Bluetooth, WLAN, WiMAX and UWB. In addition, wireless systems have been commonly used for different purposes such as radar and biomedical applications in UWB and X-band. For this reason, today's space and weight limited, and low cost portable devices must be compatible with the above systems according to the purpose, and hence they require a multiband or a wideband antenna [1–4]. Frequency designations are presented in Table 1 for convenience.

A planar monopole antenna (PMA) is simply generated by replacing a monopole above the ground plane with a planar radiator sheet. Many different kinds of geometries of planar monopoles have been proposed for various applications since its first introduction by Dubost and Zisler [5]. PMAs provide wide bandwidth with very fine control and less degradation on the radiation pattern with an acceptable gain in the band [4, 6]. In addition to the useful properties of PMAs, printed planar monopole antennas (PPMA) have other advantages such as small size, low weight, low cost and easy implementation. Moreover, low group delay deviation of PPMAs makes them suitable for pulse based systems such as UWB which has recently received great attention from industry. UWB provides more accuracy than the conventional systems especially for through-wall imaging, localization and biomedical diagnostics. UWB also offers very high data rate, multipath fading immunity and high resistance to jamming in short-range communication [7]. However, UWB may suffer from coupling and interference with Bluetooth, WLAN and WiMAX [8]. As a result, their effects in UWB must be suppressed, but the suppression degrades the pulse based system performance, e.g., communication, radar and biomedical diagnostic systems. Therefore, in this study, it is intended to design and implement a wideband PPMA to cover PCS, UWB and X-band by decreasing the coupling effects with the suppression of Bluetooth and commonly used WLAN band and WiMAX bands, the ones allocated out of UWB.

Received 3 September 2015, Accepted 27 November 2015, Scheduled 9 December 2015

* Corresponding author: Goksenin Bozdag (gokseninbozdag@iyte.edu.tr).

The authors are with the Department of Electrical and Electronics Engineering, Izmir Institute of Technology, Izmir 35430, Turkey.

Table 1. Frequency designations from PCS to X-Band.

Band Designation	Frequency (GHz)	
Public Communication System (PCS)	1.710–1.784	(uplink)
	1.805–1.879	(downlink)
Bluetooth	2.400–2.485	(802.15.1)
WLAN (common)	2.412–2.472	(802.11/a-n)
WLAN (optional)	3.657–3.690	(802.11y)
	4.942–4.948	(802.11/a-j)
	5.180–5.825	(802.11/a-n)
WiMAX	2.4, 5.8	(unlicensed)
	2.5, 3.5	(licensed)
Ultra Wide Band (UWB)	3.1–10.6	(802.15.3)
X-band	8.0–12.0	(Radar and Biomedical Apps)

2. ANTENNA DESIGNS, RESULTS AND COMPARISONS

In the design of a PPMA, radiating patch and feeding line are the main components. Microstrip [9–14] and coplanar waveguide [15–20] structures are generally employed for feeding PPMAs. Even though various geometries have been used for the radiating patch in different applications [12, 13, 16, 18], tapered geometries are frequently used in order to obtain wide bandwidth, almost constant gain and group delay. Although there are also some studies proposing a general design procedure for specific type of PPMAs [21, 22], there is no exact formulation in the literature, and the designs are generally optimized by employing computational parametric studies. In this study, it is intended to design a PPMA operating in PCS, UWB and X-band, and microstrip feeding with partial ground is preferred because of its easy implementation and simple design. First of all, a trapezoidal geometry is employed as a radiating patch, and then the dimensions of radiating patch, feeding line and ground plane are optimized. The feeding gap between ground plane and radiator patch is another critical parameter which must be taken into consideration [4, 16, 21]. Parametric studies are very useful for understanding the effects of parameters on the performance of antennas. However, individual parametric studies are not enough to obtain desired antenna characteristic,s and all of the parameters must be optimized systematically. Comprehensive numerical studies with parametric analysis have been performed by using HFSS to obtain the optimum designs before the fabrications and the measurements, and CST was also used for comparison purposes. When the physical size constraints are taken into account, the maximum widths of the radiator patch and ground plane are chosen as to be equal to each other, and width (W_3) is set to 35 mm as seen in Figure 1. The length of the ground plane (L_g) can be determined via the empirical formula obtained by the comparisons of the computational and experimental results, and it is given as $L_g \geq \lambda_{\max}/(5.35\sqrt{\epsilon_r})$ where $\lambda_{\max}$ is the maximum wavelength in the band. To make the total antenna length (L_t) as small as possible for its usage in PCS applications, L_g is chosen as 20 mm accordingly. The width of the feeding line (W_f) is chosen as 3.56 mm to obtain a 50 Ω characteristic line impedance. The other dimensions are determined by means of bottom-to-up strategy whose main purpose is to improve the impedance matching and its operation steps are summarized as follow [23–25]. Firstly, the overall dimensions of the antenna are fixed, then the structure is divided into separate sections ordered by starting from the feeding. The role of each section and its influence on impedance matching are identified. Then, the dominant parameters which will be used for further optimizations are determined for each section. The optimization process is started from the lowermost section and finalized at the uppermost one. During the process, if interested parameter is a common parameter for two sections, the parameter is optimized for the upper section.

Therefore, the antenna geometry shown in Figure 1(a) is divided into three design sections, two tapered transitions and a radiator, and the resulting antenna is called preliminary PPMA. Two

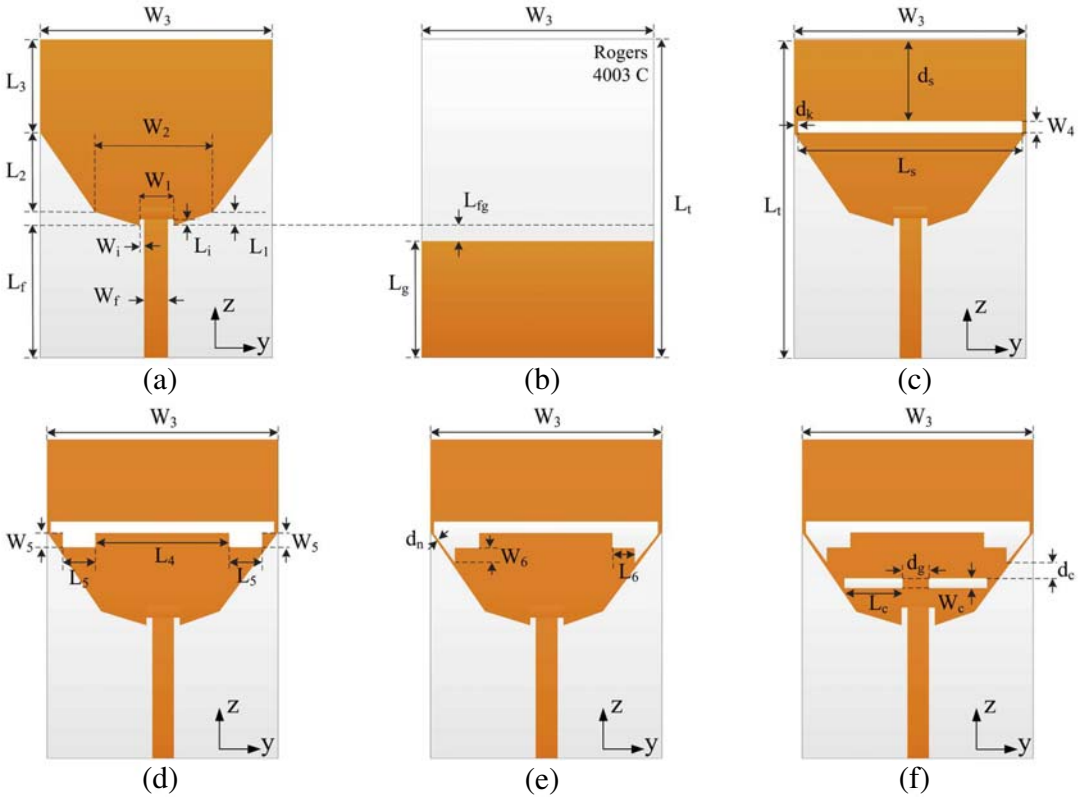

Figure 1. Geometry of PPMAs (a) Front view of preliminary PPMA with $W_1 = 4.06$, $L_1 = 1.75$, $W_2 = 18$, $L_2 = 13$, $W_3 = 35$, $L_3 = 13$, $W_f = 3.56$, $L_f = 20.1$, $W_i = 0.25$, $L_i = 0.75$. (b) Back view of the PPMAs with $L_g = 20$, $L_{fg} = 0.1$, $L_t = 47.85$. (c) The first stage of the proposed PPMA with $d_s = 13.55$, $d_k = 0.5$, $L_s = 34$, $W_4 = 1.6$. (d) The second stage of the proposed PPMA with $L_4 = 20.8$, $W_5 = 2$, $L_5 = 5.25$. (e) The third stage of the proposed PPMA with $W_6 = 2.5$, $L_6 = 3.5$, $d_n = 0.35$. (f) The final stage of the proposed PPMA with $d_c = 3$, $W_c = 1$, $L_c = 9$, $d_g = 4$ (all dimensions are in mm).

tapered transition sections provide smooth impedance transition between the feeding line and radiation section [23, 24]. The first tapered transition section, which is the one adjacent to the feed line, is the most sensitive part, and therefore, this section must be optimized first to get desired impedance bandwidth. The resulting widths and length of the first transition section are $W_1 = 4.06\,\text{mm}$, $W_2 = 18\,\text{mm}$, and $L_1 = 1.75\,\text{mm}$, respectively. The second tapered transition section is employed to increase the bandwidth. The tapering angles of the two tapered sections are different. The widths of the second transition section are $W_2 = 18\,\text{mm}$ and $W_3 = 35\,\text{mm}$, and the length of that section is optimized as $L_2 = 13\,\text{mm}$. The length of the radiation section has a significant effect on the minimum operating frequency of the antenna, and the length of this section is optimized as $L_3 = 13\,\text{mm}$ to obtain the desired frequency range. Additionally, the length of the feeding gap is optimized as $L_{fg} = 0.1\,\text{mm}$ to improve impedance matching. L_{fg} and L_g are presented in Figure 1(b). Moreover, in order to obtain better impedance matching, an inset is also employed, and its length and width are optimized as $L_i = 0.75\,\text{mm}$ and $W_i = 0.25\,\text{mm}$, respectively. Finally, the width and length of the antenna are obtained as $W_3 = 35\,\text{mm}$ and $L_t = 47.85\,\text{mm}$, respectively. The computed VSWR result of the preliminary antenna ($L_3 = 13\,\text{mm}$) is presented in Figure 2. As seen from the figure, it has an operating bandwidth of 10.5 GHz with frequency range of 2–12.5 GHz, which does not cover PCS. To cover PCS band, the length of the radiation section L_3 is increased from its original value 13 mm to 15.65 mm step by step, and the results are given in Figure 2. It is seen from the figure that the minimum operating frequency slightly decreases with increasing L_3, and it is not possible to cover PCS band by only increasing L_3. L_3 is chosen as 15.15 mm to limit the total length L_t to 50 mm which is 2.15 mm longer than the total length of the preliminary antenna.

Implementation of proper slots having specific locations on an antenna is generally used for the excitation of additional operating frequencies [15, 18, 19, 26], band stopping [11, 13, 16, 17, 20, 21], antenna miniaturization [10, 26], gain and bandwidth enhancements [9, 12, 14]. Therefore, slots are employed on preliminary PPMA in order to cover PCS and to suppress Bluetooth, WLAN (2.45 GHz) and WiMAX (2.4 and 2.5 GHz) and thus to obtain final design, the proposed PPMA. The antenna geometries with slots, used to obtain the proposed antenna, are presented in Figure 1(c) through Figure 1(f). A rectangular slot shown in Figure 1(c) is firstly employed, and the effects of the changes in its dimensions are examined in terms of the excitation of PCS band. The effects of the length and width of the slot are given in Figure 3 and Figure 4, respectively. As seen from Figure 3, using a rectangular slot shifts the minimum operating frequency to lower frequencies and rejects the band around 3 GHz. It is also seen from the figure that the minimum operating frequency of the excited band around 2 GHz decreases slightly, and its bandwidth becomes narrower by increasing the length of the slot. The width of the rectangular slot also affects the minimum operating frequency and the bandwidth as presented in Figure 4, but its effect is very limited compared with the effect of length. From the parametric studies above, it is seen that Bluetooth, WLAN and WiMAX bands are suppressed by implementing a rectangular slot, but it is not possible to cover PCS band.

Since the edge of the transition sections are more sensitive, small rectangular slots shown in Figure 1(d) and a triangle slot shown in Figure 1(e) are located closer to the edge of the second transition section. Their geometries and positions are optimized to cover desired PCS band, and the results are presented in Figure 5. On the other hand, these modifications deteriorate the impedance matching around 7.5 GHz. To overcome this problem, the effect of the length of the inset is examined in Figure 6. Impedance matching around 7.5 GHz is achieved by choosing $L_i = 1.5$ mm, which decreases

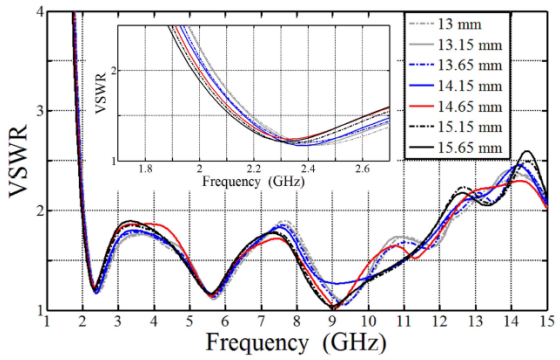

Figure 2. Figure 1(a) with various values of L_3.

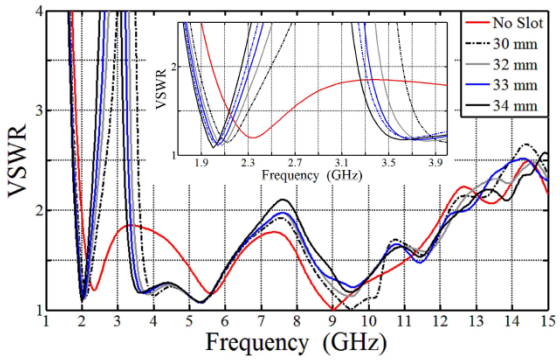

Figure 3. Figure 1(c) with various values of L_s ($L_3 = 15.15$ mm, $W_4 = 1.6$ mm, $d_s = 13.55$ mm).

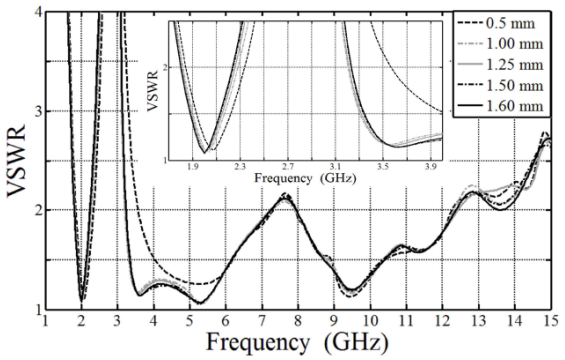

Figure 4. Figure 1(c) with various values of W_4 ($L_s = 34$ mm, $d_k = 0.5$ mm).

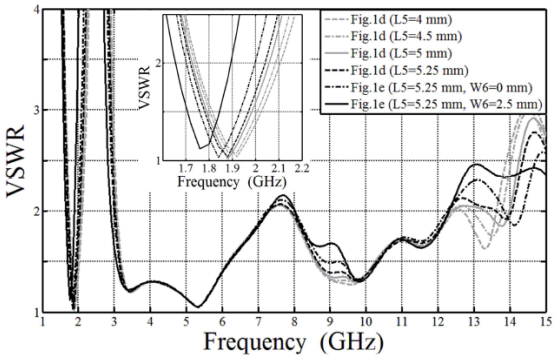

Figure 5. Figure 1(d) and Figure 1(e) with various values of L_5 and W_6 ($L_4 = 20.8$ mm, $W_4 = 1.6$ mm, $W_5 = 2$ mm).

the maximum operating frequency below 12 GHz. To increase the maximum operating frequency, compensation slots [9] are implemented and located symmetrically on the second transition section as seen in Figure 1(f). The effects of these slots are presented in Figure 7, and d_g is chosen as 4 mm to increase the upper frequency limit above 12 GHz. The antennas were realized according to the optimum results obtained from the parametric studies presented above. They are fabricated by using photolithography and commercially available substrate Rogers 4003C whose relative dielectric constant (ϵ_r), tangent loss and thickness are 3.55, 0.0027 and 1.524 mm, respectively. The fabricated preliminary and proposed PPMAs are shown in Figure 8(a) and Figure 8(b), respectively. The computed and measured VSWR results of the preliminary and proposed PPMAs are presented in Figure 9. As seen from the figure, the preliminary antenna has an operating bandwidth of 10.5 GHz with frequency range of 2–12.5 GHz according to computed results, and the measured one is 9.63 GHz with frequency range of 2.37–12 GHz (5 : 1). Even though the preliminary antenna covers Bluetooth, WLAN, WiMAX, UWB and X-band, it does not cover PCS band. According to the computed results of the proposed antenna, it is observed that the two operating bands are 1.66 GHz–1.89 GHz and 2.88 GHz–12 GHz. In the measured results, it is seen that the bands are 1.67 GHz–1.91 GHz and 12 GHz with frequency range of 3 GHz–15 GHz (5 : 1), which make the antenna suitable for PCS, UWB and X-band. The computed and measured results are in good agreement especially at lower frequencies, and the measured maximum operating frequency of the proposed antenna is much higher than the computed one. On the other hand, it is seen that the results are not in very good agreement above 9 GHz. To reveal the reason for this disagreement, the effect of the dielectric constant is examined by using HFSS and CST, and those computed results are compared with the measured one for the proposed PPMA in Figure 10.

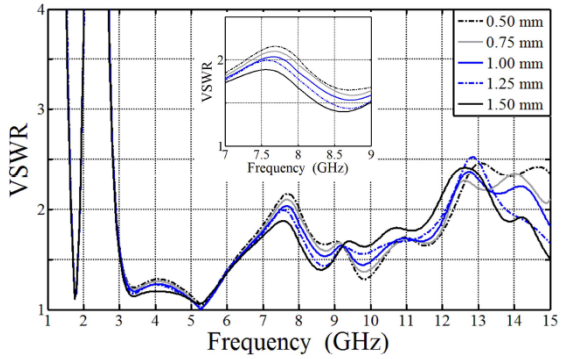

Figure 6. Figure 1(e) with various values of L_i ($L_5 = 5.25$ mm, $W_6 = 2.5$ mm).

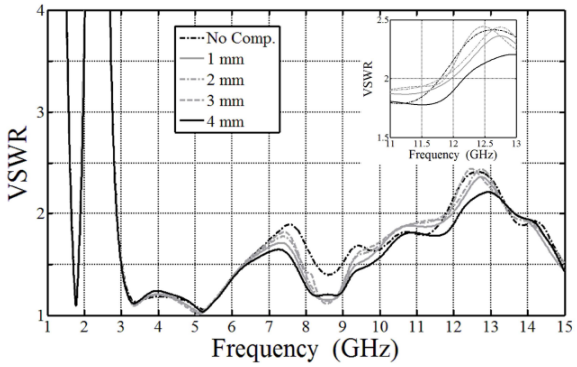

Figure 7. Figure 1(f) with various values of d_g ($L_c = 9$ mm, $W_c = 1$ mm, $L_i = 1.5$ mm).

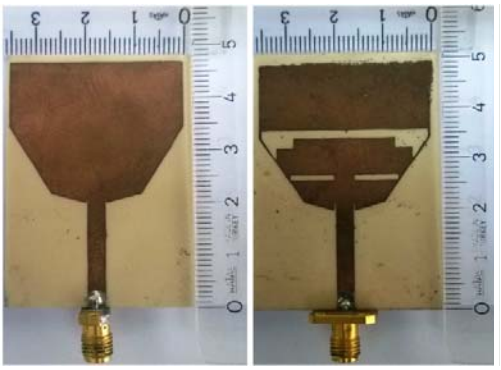

Figure 8. Fabricated PPMAs. (a) Preliminary. (b) Proposed.

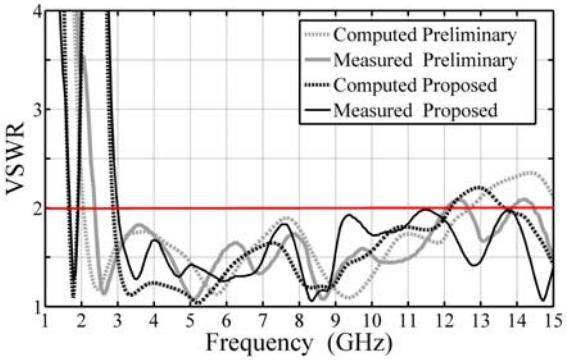

Figure 9. VSWRs of preliminary and proposed PPMAs.

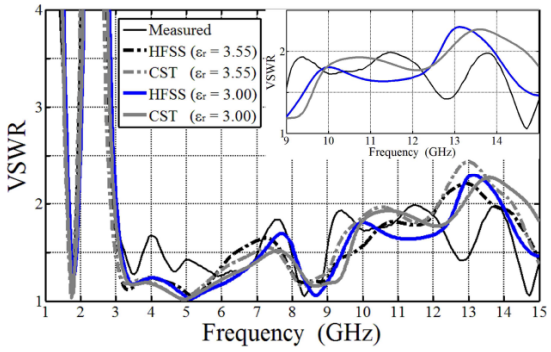

Figure 10. Comparisons and the examination of the dielectric constant for the proposed PPMA.

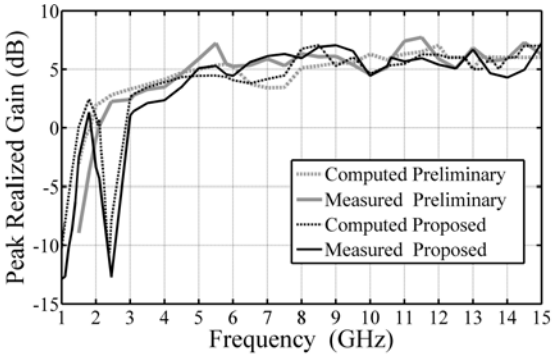

Figure 11. Peak realized gains of preliminary and proposed PPMAs.

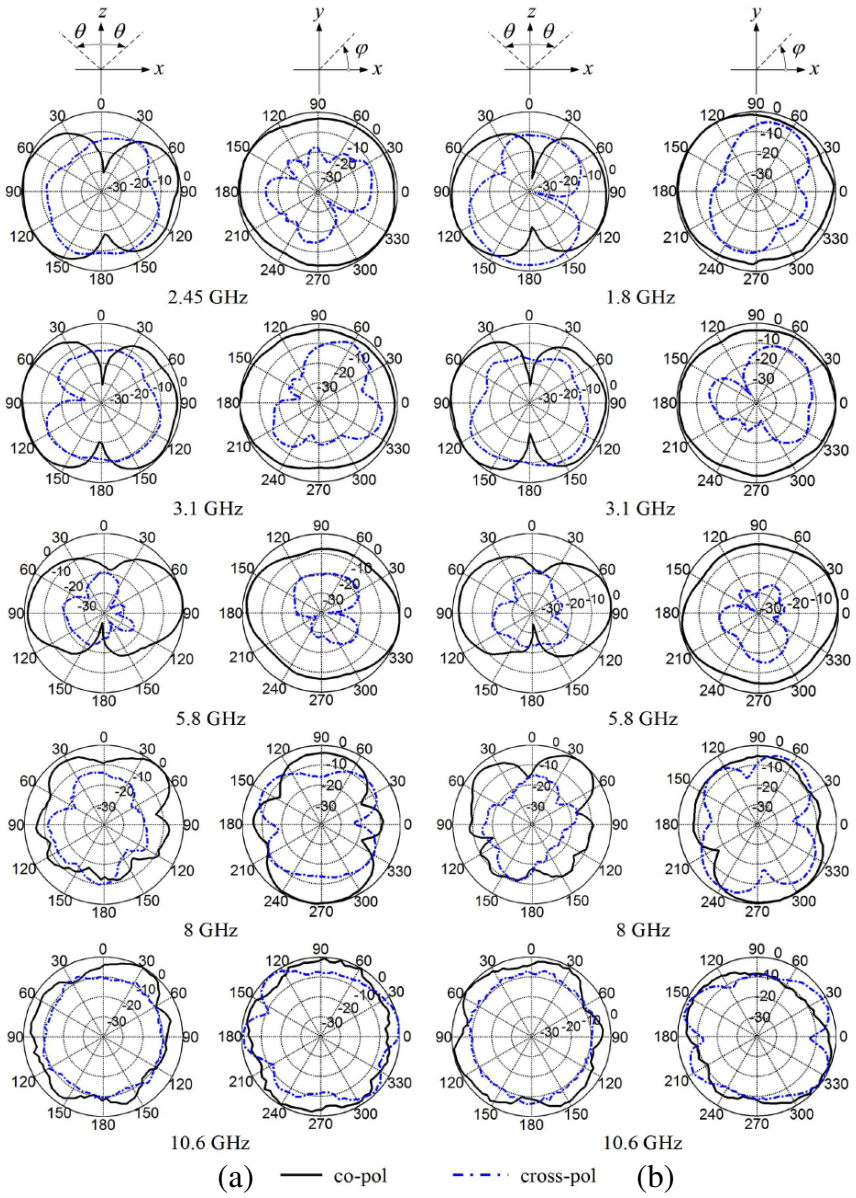

Figure 12. Measured normalized radiation patterns of PPMAs. (a) Preliminary. (b) Proposed.

According to the figure, the computed results for $\epsilon_r = 3.00$ above 9 GHz have the same type of behavior as the measured one. It can also be observed that the measured result between 9–13 GHz seems as the contracted version of the computed results for $\epsilon_r = 3.00$ between 9–15 GHz, especially if the result for HFSS is considered. Therefore, it can be concluded that there is an uncertainty in the value of the dielectric constant of the substrate at high frequencies even though that value is given as 3.55 over a very wide frequency range in the data sheet. The performances of the designed PPMAs are examined in terms of realized gain, radiation pattern and group delay as well. The antenna gains used in the calculation of measured results were obtained by the two-antenna method presented in [27]. The computed and measured peak realized gains (G_{pr}) of the PPMAs are given in Figure 11. According to the figure, the maximum value of the measured G_{pr} of preliminary PPMA reaches 7.72 dB at 11.5 GHz, and its average value is 4.95 dB in the operating band. The maximum value of measured G_{pr} of the proposed PPMA is 7.25 dB at 15 GHz. At 1.8 GHz, which represents PCS, the measured G_{pr} is 1.32 dB, and the average measured G_{pr} is 5 dB in the 3–15 GHz band. It is seen from the figure that the computed and measured peak realized gains are in good agreement for both of the antennas. The measured normalized co- and cross-polarization patterns of the preliminary and proposed PPMAs are presented in Figure 12. It is observed from the figure that the radiation patterns of PPMAs, especially the ones at lower frequencies, are almost omnidirectional in x-y plane. One can also see that cross polarization discrimination levels are 10 dB or higher in the x direction at low frequencies, but these levels decrease at high frequencies. Group delay τ_g is another parameter used to examine the time delay of signal while transmitting through a device. It is given by $\tau_g = -d\phi/d\omega$ where ϕ is the phase response of signal and ω the angular frequency. Although constant group delay is desired to avoid signal distortions for transmission, it is not generally possible in applications, and small deviations are acceptable. The comparisons of simulated and measured group delay performances of preliminary and proposed PPMAs are presented in Figure 13 and Figure 14, respectively. Since the group delay performance of the antenna has a critical role especially in pulse based communication applications, it was examined for only UWB. CST was used to simulate group delays, and the measured ones were obtained by using the method given in [28]. The antennas were placed 20 cm away from each other. As can be seen from Figure 13 and Figure 14, the preliminary and proposed PPMAs have maximum group delay deviations of 1 ns and 1.25 ns, respectively. It can be said that the group delay performances of the antennas are good for UWB applications.

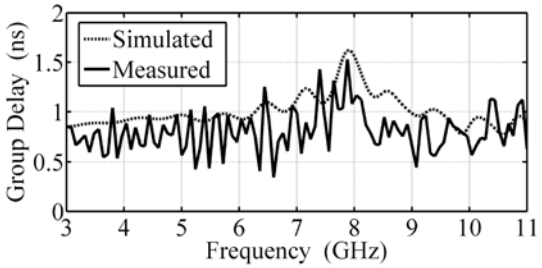

Figure 13. Simulated (CST) and measured group delays of preliminary PPMA.

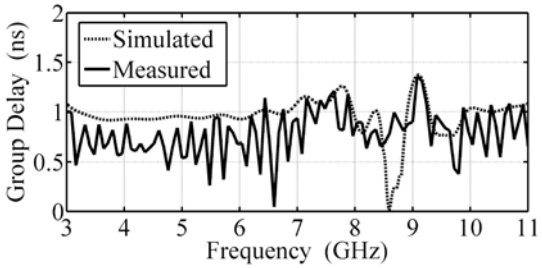

Figure 14. Simulated (CST) and measured group delays of proposed PPMA.

3. CONCLUSION

In this study, a printed planar monopole antenna has been designed and realized for PCS, UWB and X-Band applications. The design procedure includes two stages. In the first one, a preliminary PPMA was investigated by employing bottom to up strategy, and it was divided into sections which were optimized to obtain broader bandwidth. The resulting antenna operates in the 2.37–12 GHz band with an average peak realized gain of 4.95 dB, and therefore, it can be considered as a PPMA which is suitable for Bluetooth, WLAN, WiMAX, UWB and X-band. In the second stage, slots were implemented on the preliminary PPMA to suppress Bluetooth, WLAN, WiMAX and to excite PCS. As a result, the proposed antenna operates in the 1.67–1.91 GHz band, where PCS is allocated, and the 3–15 GHz band,

where UWB and X-band are allocated. The measured group delays of the preliminary and proposed PPMAs are satisfactory with maximum 1 ns and 1.25 ns deviations in the whole UWB, respectively. Consequently, the proposed antenna is a good candidate for wideband, multipurpose and portable devices.

REFERENCES

1. Vainikainen, P., et al., "More than 20 antenna elements in future mobile phones, threat or opportunity?" *3rd European Conference on Antennas and Propagation*, 2940–2943, Berlin, 2009.
2. Asghar, A., M. Malick, M. Karlsson, and A. Hussain, "A multiwideband planar monopole antenna for 4G devices," *Microwave Opt. Technol. Lett.*, Vol. 55, No. 3, 589–593, 2013.
3. Praveen, S., O. Raoul, P. Bradley, A. David, L. Todd, S. Daniel, K. Jonathan, and P. John, "Miniature radar for mobile devices," *IEEE High Performance Extreme Computing Conference*, 1–8, Waltham, 2013.
4. Ammann, M., "Control of the impedance bandwidth of wideband planar monopole antennas using a beveling technique," *Microwave Opt. Technol. Lett.*, Vol. 30, No. 4, 229–232, 2001.
5. Dubost, G. and S. Zisler, *Antennas a Large Bande*, Masson, Paris, 1976.
6. Agrawall, N. P., G. Kumar, and K. Ray, "Wide-band planar monopole antennas," *IEEE Trans. Antennas Propag.*, Vol. 46, No. 2, 294–295, 1998.
7. Win, M. Z., et al., "History and applications of UWB," *Proc. IEEE*, Vol. 97, No. 2, 198–204, 2009.
8. Kim, W. C. and W. G. Yang, *Design and Implementation of UWB CPW-fed Planar Monopole Antenna with Dual Band Rejection Characteristics, Ultra Wideband Communications: Novel Trends Antennas and Propagation*, M. A. Matin (ed.), InTech, DOI: 10.5772/941, 2011.
9. Low, Z., J. Cheong, and C. Law, "Low-cost PCB antenna for UWB applications," *IEEE Antennas Wireless Propag. Lett.*, Vol. 4, 237–239, 2005.
10. Lu, Y., Y. Huang, H. T. Chattha, and Y. Shen, "Technique for minimising the effects of ground plane on planar ultra–wideband monopole antennas," *IET Microwaves Antennas Propag.*, Vol. 6, No. 5, 510–518, 2012.
11. Ojaroudi, M. and N. Ojaroudi, "Ultra–wideband slot antenna with frequency band-stop operation," *Microwave Opt. Technol. Lett.*, Vol. 55, No. 9, 2020–2023, 2013.
12. Ray, K., S. Thakur, and A. Deshmukh, "Slot cut printed elliptical UWB monopole antenna," *Microwave Opt. Technol. Lett.*, Vol. 56, No. 3, 631–635, 2014.
13. Abdollahvand, A., A. Pirhadi, H. Ebrahimian, and M. Abdollahvand, "A compact UWB printed antenna with bandwidth enhancement for in-body microwave imaging applications," *Progress In Electromagnetics Research C*, Vol. 55, 149–157, 2014.
14. Beigi, P., J. Nourinia, B. Mohammadi, and A. Valizafe, "Bandwidth enhancement of small square monopole antenna with dual band notch characteristic using U-shaped slot and butterfly shape parasitic element on backplane for UWB applications," *ACES J.*, Vol. 30, No. 1, 78–85, 2015.
15. Joseph, S., B. Paul, S. Mridula, and P. Mohanan, "CPW-fed UWB compact antenna for multiband applications," *Progress In Electromagnetics Research C*, Vol. 56, 29–38, 2015.
16. Parkash, D. and R. Khanna, "Triple band rectangular-shaped monopole antenna for WLAN/WiMAX/UWB applications," *Microwave Opt. Technol. Lett.*, Vol. 52, No. 9, 2540–2544, 2010.
17. Zehforoosh, Y. and T. Sedghi, "A CPW-fed printed antenna with band-notched function using an M-shaped slot," *Microwave Opt. Technol. Lett.*, Vol. 56, No. 5, 1088–1092, 2014.
18. Xu, Y., C. Zhang, Y.-Z. Yin, and Z. Yang, "Compact triple-band monopole antenna with inverted-L slots and SRR for WLAN/WiMAX applications," *Progress In Electromagnetics Research Letters*, Vol. 55, 1–6, 2015.
19. Wu, R., P. Wang, Q. Zheng, and R. Li, "Compact CPW-fed triple band antenna for diversity applications," *Elect. Lett.*, Vol. 56, No. 10, 735–736, 2015.

20. Bakariya, P. S., S. Dwari, and M. Sarkar, "Triple band notch UWB printed monopole antenna with enhanced bandwidth," *Int. J. Elect. Comm. (AEÜ)*, Vol. 69, 26–30, 2015.
21. Wang, J. and X. He, "Analysis and design of a novel compact multiband printed monopole antenna," *Int. J. Antennas Propag.*, Article ID 694819, 2013.
22. Ray, K. P. and S. Thakur, "Ultra wide band vertex truncated printed pentagon monopole antenna," *Microwave Opt. Technol. Lett.*, Vol. 56, No. 10, 2228–2234, 2014.
23. Tran, D., *On the Design of a Super Wideband Antenna, Ultra Wideband*, B. Lembrikov, ed., InTech, DOI: 10.5772/941, 2010.
24. Tanyer-Tigrek, F. M., D. P. Tran, I. E. Lager, and L. P. Ligthart, "CPW-fed quasi-magnetic printed antenna for ultra-wideband applications," *IEEE Antennas Propag. Magazine*, Vol. 51, No. 2, 61–70, 2009.
25. Manohar, M., U. K. Nemani, R. S. Kshetrimayum, and A. K. Gogoi, "A novel super wideband notched printed trapezoidal monopole antenna with triangular tapered feedline," *International Conference on Signal Processing and Communication*, 1–6, Bangolore, 2014.
26. Latif, S. I., L. Shafai, and S. K. Sharma, "Bandwidth enhancement and size reduction of microstrip slot antennas," *IEEE Trans. Antennas Propag.*, Vol. 53, No. 3, 994–1003, 2005.
27. Balanis, C. A., *Antenna Theory: Analysis and Design*, Wiley, Hoboken, 2012.
28. McEvoy, P., M. John, S. Curto, and M. J. Ammann, "Group delay performance of ultra wideband monopole antennas for communication applications," *Antennas and Propagation Conference*, 377–380, Loughborough, 2008.